



Title	Scaffold-Free Tissue-Engineered Construct-Hydroxyapatite Composites Generated by an Alternate Soaking Process : Potential for Repair of Bone Defects
Author(s)	Matsusaki, Michiya; Kadowaki, Koji; Tateishi, Kosuke et al.
Citation	TISSUE ENGINEERING: Part A. 2009, 15(1), p. 55-63
Version Type	VoR
URL	https://hdl.handle.net/11094/50783
rights	© Mary Ann Liebert, Inc.
Note	

The University of Osaka Institutional Knowledge Archive : OUKA

<https://ir.library.osaka-u.ac.jp/>

The University of Osaka

Scaffold-Free Tissue-Engineered Construct–Hydroxyapatite Composites Generated by an Alternate Soaking Process: Potential for Repair of Bone Defects

Michiya Matsusaki, Ph.D.,^{1,2} Koji Kadowaki, M.S.,¹ Kosuke Tateishi, M.D., Ph.D.,³
Chikahisa Higuchi, M.D., Ph.D.,³ Wataru Ando, M.D., Ph.D.,³ David A. Hart, M.D., Ph.D.,⁴
Yoshinari Tanaka, M.D., Ph.D.,^{2,3} Yasuhiro Take, M.D.,³ Mitsuru Akashi, Ph.D.,^{1,2}
Hideki Yoshikawa, M.D., Ph.D.,^{2,3} and Norimasa Nakamura, M.D., Ph.D.^{2,3}

Mesenchymal stem cell (MSC)–based tissue-engineered construct (TEC)–hydroxyapatite (HAp) composites were developed by an alternate soaking process. The TEC derived from cultured synovial MSCs was alternately immersed in varying concentrations of $\text{CaCl}_2/\text{Tris-HCl}$ and $\text{Na}_2\text{HPO}_4/\text{Tris-HCl}$ buffers, and HAp formation was analyzed by Fourier transform infrared spectroscopy (FT-IR), wide-angle X-ray diffraction, and scanning electron microscopy (SEM). These analyses clearly demonstrated HAp formation in the TEC. Specifically, SEM assessments showed that spherical HAp crystals of $\sim 1\ \mu\text{m}$ were directly formed on the surfaces of the cells and extracellular matrix (ECM) fibers. Cytotoxicity from exposure to calcium or phosphate buffers of $>100\ \text{mM}$ concentrations as assessed by LIVE/DEAD staining and total DNA assays was detected, but such cytotoxicity was not detected following exposure to concentrations of $<50\ \text{mM}$. The HAp nanocrystals (ca. $\sim 500\ \text{nm}$) were formed after 20 cycles in $10\ \text{mM}$ calcium or phosphate buffers, and cell survival in the composites was confirmed. Moreover, preliminary implantation of TEC-HAp composites derived from rabbit synovial MSCs to rabbit osteochondral defects exhibited accelerated osteoinduction. These composites may be the first example of a hybrid material that consists of ECM, HAp nanocrystals, and living MSCs, and the TEC-HAp composite could be a unique and useful material for bone tissue engineering.

Introduction

IN CLINICAL SETTINGS, autologous bone grafts are widely used to repair defects; however, mismatch in size between the donor and recipient site, and moreover potential risk of donor site morbidity may limit their use. A number of biomaterials have been developed for potential use in bone tissue engineering. Hydroxyapatite (HAp), $\text{Ca}_{10}(\text{PO}_4)_6(\text{OH})_2$, is one of the more attractive materials for such artificial bone applications because of its biocompatibility, the absence of inflammatory or foreign body responses, and the fact that it is of similar crystalline phase as bone mineral.^{1,2} However, a disadvantage of HAp is its mechanical properties, such as higher stiffness, brittleness, and crystallinity, as compared with natural bone, which give rise to concerns with regard to clinical use. Thus, researchers have studied hybrid materials composed

of HAp and polymeric biomaterials, such as poly(L-lactic acid),³ poly(lactic-co-glycolic acid),⁴ cellulose,^{5,6} gelatin,^{7,8} poly(ethylene glutarate),⁹ and collagen,^{10,11} to modify its mechanical properties and functionality. However, the use of these polymeric materials still carries risks of long-term side effects, such as immunogenicity, disease transmission, or inflammation during the hydrolysis process in the transplanted sites.¹² In order to avoid such unknown risks, polymeric materials should be minimally combined with HAp. One interesting option in this quest to enhance bone formation is a combination of mesenchymal stem cells (MSCs) with a HAp-based scaffold. Adding bone marrow–derived MSCs directly with a HAp scaffold has been studied, and a positive effect of MSCs on osteogenic capacity has been demonstrated.¹³ An obvious next step would be the development of a HAp-based hybrid material in combination with a more natural MSC-generated matrix.

¹Department of Applied Chemistry, Graduate School of Engineering, Osaka University, Suita, Osaka, Japan.

²21st Century COE Program "Center for Integrated Cell and Tissue Regulation," Graduate School of Engineering, Osaka University, Suita, Osaka, Japan.

³Department of Orthopaedics, Graduate School of Medicine, Osaka University, Suita, Osaka, Japan.

⁴Faculty of Medicine, McCaig Institute for Bone & Joint Health, University of Calgary, Calgary, Canada.

We have recently developed a novel scaffold-free tissue-engineered construct (TEC) composed of cultured MSCs and the extracellular matrices (ECMs) produced by the cells.¹⁴ TEC containing MSCs at high density exhibited an efficient osteogenic differentiation capability (W. Ando *et al.*, submitted), and therefore such TEC may be starting point for further development of a potential material for bone tissue engineering. However, the TEC requires a specific osteoinductive growth medium or supplementation with humoral factors such as bone morphogenetic protein (BMP) for the osteoinduction *in vitro* (W. Ando *et al.*, unpublished data). As the biological activity and safety of growth factors such as BMP are not completely known yet, alternative methods to stimulate osteoinduction of TEC are needed.

Taguchi *et al.* and Akashi and colleagues discovered an alternate soaking process to simply and rapidly create bone-like HAp on/in polymeric and metal materials (Fig. 1).^{15–19} HAp formation by this alternate soaking process was approximately 100 times faster than that of a biomimetic process in simulated body fluid.²⁰ Further, HAp–agarose gel composites created by such an alternate soaking process had low crystallinity and biodegradability, but effective osteoinduction properties in periodontal tissue regeneration studies *in vivo*.^{17,19} In an extension of this approach, we hypothesized that application of an alternate soaking process to a previously described TEC would lead to development of TEC–HAp composites that would enhance the osteoinductive properties of a basic TEC.

In the present study, HAp crystals were deposited on the surface of TEC generated from human synovial MSCs using an alternate soaking process, and the process was optimized by controlling the concentration of calcium/Tris–HCl and phosphate/Tris–HCl buffers. Analogous TEC–HAp composites derived from rabbit synovial MSCs exhibited enhanced osteoinductive properties in preliminary *in vivo* implantation studies to repair osteochondral defects. Therefore, such TEC–HAp composites represent a unique material for bone tissue engineering and also for specific stem cell therapy.

Materials and Methods

Materials

All reagents were of the highest quality available and used as purchased without further purification. Calcium chloride (CaCl_2), disodium hydrogenphosphate (Na_2HPO_4), and 2-amino-2-hydroxymethyl-1,3-propanediol hydrochloride (Tris–HCl) were purchased from Wako Pure Chemical Industries (Osaka, Japan). L-Ascorbic acid 2-phosphate (Asc 2-P) was purchased from Sigma (St. Louis, MO). Solutions of these chemicals were used after filtration for steriliza-

tion. High-glucose Dulbecco's modified Eagle's medium (DMEM), Penicillin/Streptomycin, and trypsin–EDTA (0.25% trypsin and 1 mM EDTA) were purchased from Gibco BRL, Life Technologies (Rockville, MD). Collagenase for human synovium was purchased from Worthington Biochemical (Lakewood, NJ). Fetal bovine serum (FBS) was purchased from Hyclone (Logan, UT). All other chemicals were purchased from Nakarai Tesque (Kyoto, Japan).

Harvest of synovial tissue and isolation of MSCs

The harvesting and isolation of synovial cells were performed based on our previous report.¹⁴ Briefly, human synovial membranes from four male patients (average 28.8 [26–33] years old) were obtained from arthroscopic surgeries of the knee in accordance with a protocol approved by the institutional ethical committee. Rabbit synovial membranes were also obtained aseptically from the knee joints of the rabbit (male, 3 months old), postmortem within 12 h of death and with institutional ethics approval. Synovial membrane specimens of both species were rinsed with calcium- and magnesium-free phosphate-buffered saline (PBS), minced meticulously, and digested with 0.2% collagenase (Worthington Biochemical) for 1.5 h at 37°C. After neutralization of the collagenase by growth medium containing high-glucose DMEM (Gibco BRL) supplemented with 10% FBS (Hyclone) and Penicillin/Streptomycin (Gibco BRL), the cells were collected by centrifugation, washed with PBS, resuspended in the growth medium, and plated in a T-25 culture flask.

For expansion, the cells were cultured in the growth medium at 37°C in a humidified atmosphere of 5% CO_2 . The medium was replaced once per week. After 15–28 days of primary culture, when the cells reached confluence, they were washed with PBS, harvested by treatment with trypsin–EDTA (Gibco BRL), and replated at a 1:3 dilution for the first subculture. The cell passages were continued in the same manner with 1:3 dilutions when the cells reached confluence. Cells at passages 4 to 7 were used in this study. We have previously confirmed that the obtained human synovial cells possessed the characteristics of MSCs, such as cell surface antigen phenotype, renewal capacity, and pluripotency,¹⁴ and accordingly the cells were designated to be synovial MSCs.

Development of the basic TEC

The synovial MSCs (passage = 5) were seeded onto six-well culture dishes at a density of 4.0×10^5 cells/cm² in growth medium with 0.2 mM Asc 2-P. After 7 days of cell culture, a monolayer complex of cultured cells and ECM produced by these cells was detached from the dish by the application of a shear stress using gentle pipetting. The detached monolayer complex was left in suspension to form a three-dimensional (3D) structure by active tissue contraction. This tissue was termed a basic scaffold-free 3D TEC.¹⁴

Alternate soaking protocol for TEC

The alternate soaking process was performed to form HAp on the surface of the TEC as shown in Figure 1. At the first step, the TEC from six-well culture dishes was soaked in 10 mL of 10–200 mM CaCl_2 /50 mM Tris–HCl buffer (pH = 7.4) at room temperature for 10 s, and washed to re-

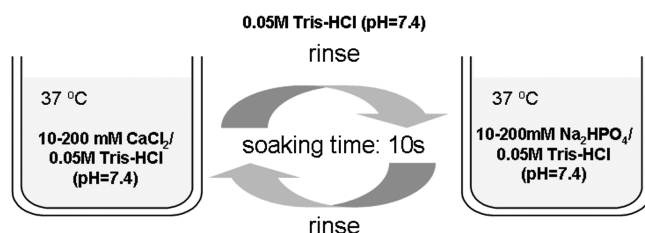


FIG. 1. Scheme of the alternate soaking process used in this study.

move excess calcium ions by immersion in 10 mL of 50 mM Tris-HCl buffer (pH = 7.4) for 10 s. Next, the TEC was soaked in 10 mL of 10–200 mM Na_2HPO_4 /50 mM Tris-HCl buffer (pH = 7.4) at room temperature for 10 s and washed with 10 mL of 50 mM Tris-HCl buffer (pH = 7.4) for 10 s. These steps represent one cycle. The alternate soaking process was then repeated for a variable number of cycles as outlined in specific experiments.

Characterization of the TEC-HAP composites

The TEC or TEC-HAP composites from 6-cm culture dishes were freeze-dried for 3 days in order to measure the Fourier transform infrared spectroscopy (FT-IR) spectrum, for X-ray diffraction, and for scanning electron microscopy (SEM) analyses. The IR spectrum of the dried TEC or TEC-HAP was measured using a Spectrum One FT-IR Spectrometer (Perkin Elmer Instruments, Beaconsfield, United Kingdom). The interferograms were coded 16 times and Fourier transformed at a resolution of 4 cm^{-1} . The wide-angle X-ray diffraction (WAXD) studies were recorded using an X-ray diffractometer RINT UltraX18 (Rigaku, Tokyo, Japan) equipped with a scintillation counter and using $\text{CuK}\alpha$ radiation (40 kV, 200 mA; wavelength = 1.5418 \AA), which was monochromated by a parabolic multilayer mirror in transmission geometry. The surface morphologies of the samples were observed using an SEM HITACHI S-800 (Hitachi, Tokyo, Japan).

LIVE-DEAD staining of TEC-HAP composites

To evaluate the viability of synovial MSCs after the alternate soaking process with various concentrations of calcium/Tris-HCl and phosphate/Tris-HCl buffers, the cells (passage = 7) were adhered onto a cover glass (3.0×10^4 cells/ cm^2) for 24 h and then alternately soaked for predetermined cycles. The cells were then stained by incubation in 1.0 mL of PBS containing $2\text{ }\mu\text{M}$ of calcein-AM and $4\text{ }\mu\text{M}$ of ethidium homodimer (EthD-1) (LIVE/DEAD Viability/Cytotoxicity Kit [L-3224]; Invitrogen-Molecular Probes, Carlsbad, CA) for 45 min at 37°C .²¹ The living cells stained with calcein-AM exhibit a green color, whereas dead cells stained with EthD-1 exhibit a red color by fluorescence microscopy. The fluorescence microscopic images were taken with an Olympus confocal disc scan system DSU-IX81-SET (Olympus, Tokyo, Japan).

Total DNA content of TEC after exposure to the alternate soaking process

The amount of DNA in the TEC from six-well culture dishes after alternate soaking with various concentrations of calcium/Tris-HCl and phosphate/Tris-HCl buffers was determined with a DNA assay kit (DNeasy Tissue Kit; QIAGEN, Hilden, Germany). The TEC was alternately soaked for 10 or 20 cycles in 10, 50, 100, or 200 mM CaCl_2 /50 mM Tris-HCl or Na_2HPO_4 /50 mM Tris-HCl buffer (pH = 7.4) at ambient temperature, and the DNA in the TEC was extracted. The total DNA content was subsequently measured with the DNA assay kit.

WST-1 assay of TEC-HAP composites

The survival of human synovial MSCs in TEC after exposure to the alternate soaking process was assessed by the

WST-1 assay, which is an improved version of the MTT assay.²² Briefly, $50\text{ }\mu\text{L}$ of WST-1 reagent (DOJINDO Laboratories, Kumamoto, Japan) was added to dishes containing the TEC-HAP composites from six-well culture dishes and 5 mL of Eagle's MEM (10% FBS) without phenol red, and the dishes were incubated for 3 h at 37°C . The WST-1 reagent was transformed into WST-1 formazan during the incubation by dehydrogenase that is synthesized by living cells, and thus produced the yellow-colored WST-1 formazan. The image of the TEC-HAP with yellow-colored formazan was taken using a digital still camera, DSC-F505V Cyber-shot (SONY, Tokyo, Japan).

Implantation of TEC-HAP composites derived from rabbit MSCs into osteochondral defects in vivo

Similar to the human synovial MSCs, rabbit synovial MSCs (passages 4–7) were prepared and further cultured at the density of 4.0×10^5 cells/ cm^2 with Asc 2-P in 6-cm-diameter culture dishes for 7 days, and the resultant basic TEC was prepared as allografts without any osteoinductive stimulation. TEC-HAP was prepared by 20 cycles of alternate soaking processes with 10 mM calcium/Tris-HCl and phosphate/Tris-HCl buffers. Female, one-year-old skeletally mature Japanese white rabbits ($n = 3$) were anesthetized by intramuscular injection of a mixture of ketamine hydrochloride (50 mg/mL and 0.6 mL/kg of body weight) and xylazine (20 mg/mL and 0.3 mL/kg of body weight). After a medial parapatella incision, the medial femoral condyles of both knees were exposed with the knee in deep flexion, and osteochondral defects were created that were 4.0 mm in diameter and 4.0 mm in depth using an electric router (Proxxon, Niersbach, Germany) and diamond disc grinding (Shofu, Kyoto, Japan). Subsequently, the basic TEC (to the right knee) or TEC-HAP (to the left knee) was implanted without suturing into the defect sites. Both legs were casted for immobilization for 1 week, and the rabbits were then returned to free cage activity. Six weeks post-operatively, the rabbits were euthanized under anesthesia. The femurs were dissected, and scanned using a microfocus X-ray CT system SMX-100CT-SV (Shimadzu, Kyoto, Japan) for microcomputed tomography (μCT) analysis. The data were reconstructed to produce images of the tibia, using 3D visualization and measurement software (Vay Tek).²³ After μCT analysis, the femurs were fixed and used for subsequent paraffin sectioning and histological analysis. Tissues were fixed with 4% paraformaldehyde in phosphate buffer (pH = 7.4), decalcified with EDTA, embedded in paraffin, and $4\text{-}\mu\text{m}$ sections were prepared. The sections were stained with hematoxylin and eosin.

Statistical analysis

Data were compared using one-way analysis of variance (ANOVA) with multiple comparison analysis performed using a two-sample *t*-test for each comparison with the control. *P* values less than or equal to 0.01 were considered statistically significant.

Results and Discussion

Fabrication of the TEC-HAP composite materials

HAP was deposited on the surface of human TEC using an alternate soaking process with the TEC alternately soaked in

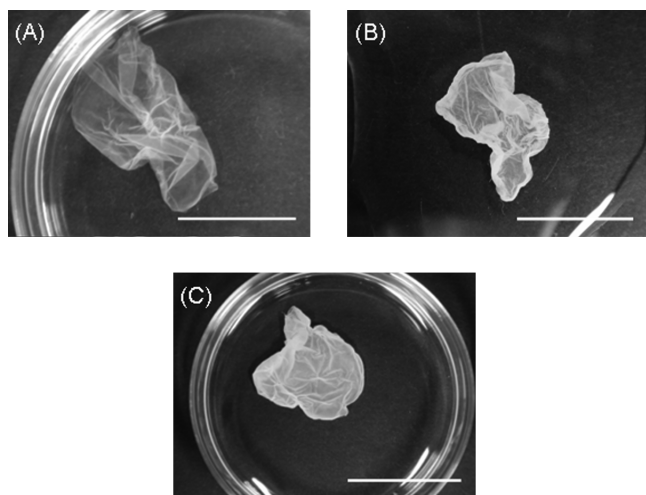


FIG. 2. Macroscopic observations of the TEC (A) before and after (B) 5 and (C) 20 cycles of alternate soaking in 200 mM CaCl_2 /50 mM Tris-HCl buffer (pH=7.4) and 120 mM Na_2HPO_4 /50 mM Tris-HCl buffer (pH=7.4). The scale bars in (A) and (B) are 1 cm, and scale bar is 2 cm in (C), respectively.

calcium/Tris-HCl and phosphate/Tris-HCl buffers for a pre-determined number of cycles. Figure 2 shows the macroscopic appearance of the TEC before and after the alternate soaking process. Although the original TEC was a transparent and soft film (Fig. 2A), it changed to a more white color depending on the number of alternate soaking cycles to which the it was exposed (Fig. 2B, C). After 20 cycles, the TEC was completely white in color and firm to touch. These observations suggested that calcium phosphate was formed on the surface of the TEC. To determine whether the crystallographic structure of the calcium phosphate was HAp, octacalcium phosphate (OCP), or β -tricalcium phosphate, the crystallographic structure of the calcium phosphate formed on the TEC was assessed by FT-IR spectroscopy and X-ray diffraction. Figure 3 shows the FT-IR spectra of the TEC before and after the alternate soaking process. The IR peaks assigned to the stretching vibration of the phosphate groups in HAp (PO_4^{3-} : 560, 600, 960, and 1095 cm^{-1}) appeared after the alternate soaking process, and the absorbance of the IR peaks increased with an increasing number of alternate soaking process cycles (Fig. 3B–D). The IR peak assigned to the stretching vibration of the phosphate groups in OCP (PO_4^{3-} : 1020 cm^{-1}) also appeared after 20 cycles of the alternate soaking process (Fig. 3D). WAXD patterns are shown in Figure 4. After alternate soaking of TEC for 0, 5, and 10 cycles, no definite diffraction peaks were observed. The definite diffraction peaks assigned to the d spacing of the HAp crystal at 10.8° (d_{100} : 8.17 Å), 21.8° (d_{200} : 4.07 Å), 22.9° (d_{111} : 3.88 Å), 25.9° (d_{002} : 3.44 Å), 31.8° (d_{211} : 2.81 Å), and 39.8° (d_{310} : 2.26 Å) were observed after 20 cycles of the alternate soaking process (Fig. 4D). The peak at 11.3° corresponding to d_{200} of OCP at 9.34 Å was also observed, but not as clearly as those for HAp. These results of the FT-IR and WAXD analyses suggest that the calcium phosphates formed on the surface of TEC were likely mainly HAp, and potentially, partly OCP. Since HAp is thermodynamically the most stable

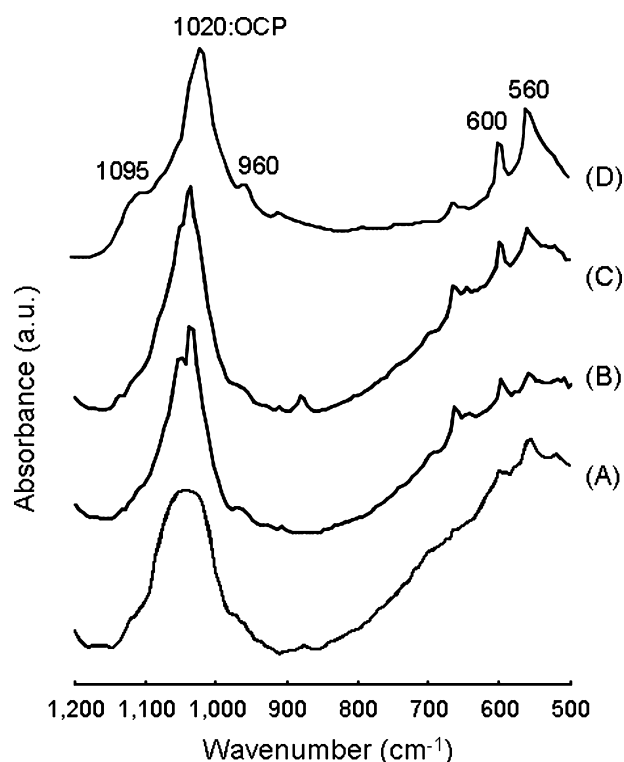


FIG. 3. FT-IR spectra of the TEC (A) before and after (B) 5, (C) 10, and (D) 20 cycles of alternate soaking in 200 mM CaCl_2 /50 mM Tris-HCl buffer (pH=7.4) and 120 mM Na_2HPO_4 /50 mM Tris-HCl buffer (pH=7.4).

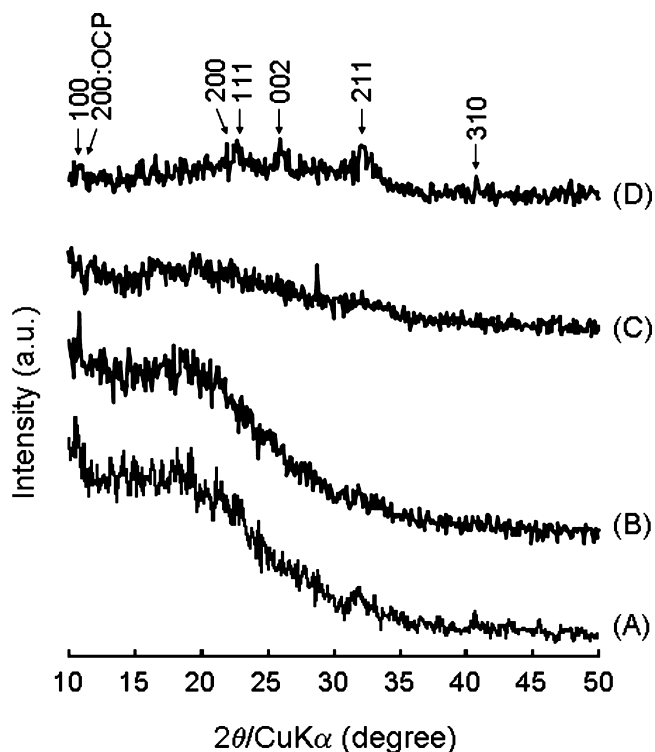


FIG. 4. WAXD patterns of the TEC (A) before and after (B) 5, (C) 10, and (D) 20 cycles of alternate soaking in 200 mM CaCl_2 /50 mM Tris-HCl buffer (pH=7.4) and 120 mM Na_2HPO_4 /50 mM Tris-HCl buffer (pH=7.4).

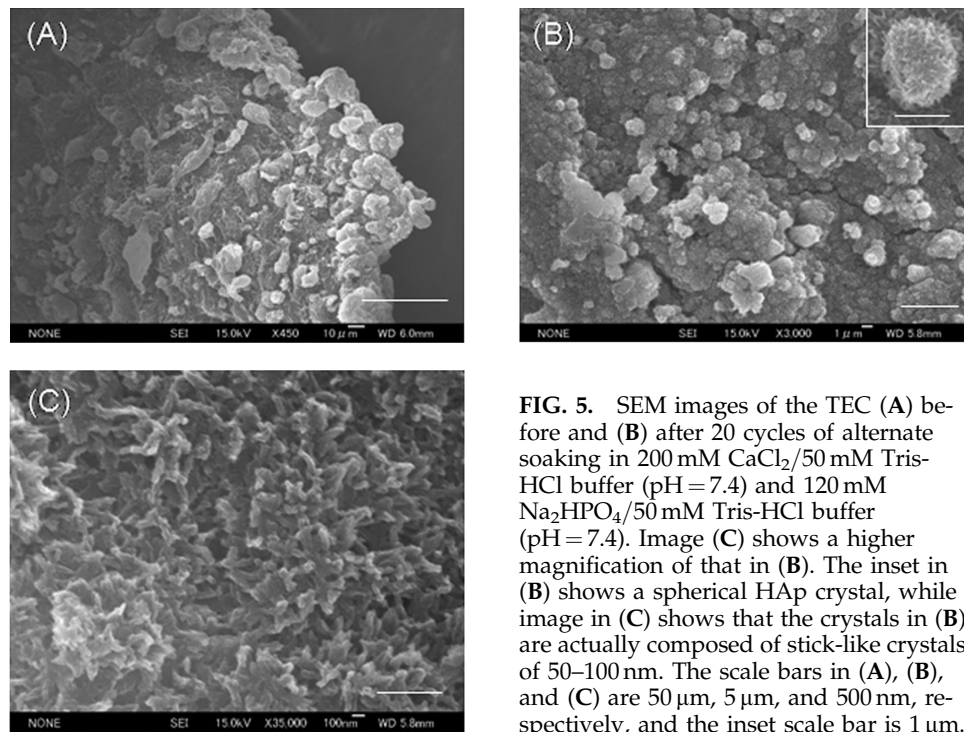


FIG. 5. SEM images of the TEC (A) before and (B) after 20 cycles of alternate soaking in 200 mM CaCl_2 /50 mM Tris-HCl buffer (pH = 7.4) and 120 mM Na_2HPO_4 /50 mM Tris-HCl buffer (pH = 7.4). Image (C) shows a higher magnification of that in (B). The inset in (B) shows a spherical HAp crystal, while image in (C) shows that the crystals in (B) are actually composed of stick-like crystals of 50–100 nm. The scale bars in (A), (B), and (C) are 50 μm , 5 μm , and 500 nm, respectively, and the inset scale bar is 1 μm .

form of calcium phosphate in a natural environment, this may explain why the predominant calcium phosphate formed on the TEC was due to HAP crystals.

The morphology of the HAP crystals formed on TEC was also assessed by SEM. Figure 5 shows SEM images of TEC before and after 20 cycles of the alternate soaking process. The original TEC was a composite film of cells and ECM fibrils (Fig. 5A), but spherical HAP crystals of approximately 1- μm diameter were observed to densely form on the TEC after the alternate soaking process (Fig. 5B). Further assessment of higher magnification images indicated that the spherical HAP crystals actually consisted of stick-like crystals of 50- to 100-nm lengths (Fig. 5C). We have previously reported spherical HAP crystal formation on/in agarose hydrogels using this alternate soaking process,^{17,24} and the sizes of the HAP crystals (ca. 200 nm) in that study were smaller than those seen in the present study. Thus, the size and morphology of the HAP crystals formed by the alternate soaking process appears to be influenced by the composition of the materials to which they adhere. In the case of a platinum plate as the substrate, irregular crystals of HAP formed on the surface of the platinum plate,¹⁸ whereas spherical HAP crystals formed on/in organic materials, such as agarose,^{17,24} poly(vinyl alcohol),¹⁶ and the TEC. A conventional HAP-polymer composite material only allows cell adhesion on the surface of the HAP crystals, and the direct formation of HAP crystals on the surface of living cells has rarely been reported. Therefore, this study may be the first report of direct HAP formation on the cell surface.

Effect of concentration of calcium and phosphate buffers on cell viability

In light of the above findings, the viability of synovial MSCs in the TEC was investigated after the alternate soaking

process. Because the HAP crystals appeared to be directly formed on the surface of the MSCs, it was possible that such HAP crystal formation could subsequently influence TEC cell viability. The viability of human synovial MSCs adhered onto a coverslip after the alternate soaking process with various concentrations of calcium/Tris-HCl and phosphate/Tris-HCl buffers was assessed by the LIVE/DEAD assay, which stains living and dead cells as green and red, respectively, on fluorescence microscopic observation. In buffer concentrations of < 50 mM, almost all cells were green, thus suggesting good survival of the cells (Fig. 6A–C). On the other hand, red-colored cells were clearly observed at buffer concentrations > 100 mM (Fig. 6D–E), indicating the presence of dead cells after only three cycles of alternate soaking in the 200 mM buffer (Fig. 6E). These results suggested that higher concentrations of calcium/Tris-HCl and phosphate/Tris-HCl buffers exert a cytotoxic effect on the cells. In order to quantitatively evaluate cell viability, a total DNA analysis of the TEC after the alternate soaking process was performed. Figure 7 shows the total DNA content of TEC after the alternate soaking process in various concentrations of calcium/Tris-HCl and phosphate/Tris-HCl buffers. As a control, we confirmed that the DNA content of TEC after immersion in only Tris buffer for 20 min (equal to elapsed time of 20 cycles) yielded nearly the same values as the original TEC without any immersion. The mean DNA content of the original TEC without any alternate soaking (0 cycle; control) was approximately 26 μg , and no statistically significant differences in total DNA content were detected after 10 or 20 cycles of alternate soaking in the 10 and 50 mM calcium and phosphate buffers. However, statistically significant decreases in DNA content were observed after exposure to the 100 mM buffer, and the DNA content of TEC decreased by > 50% after the alternate soaking process in 200 mM buffer (yields after 10 and 20 cycles were 13.4 and 5.4 μg DNA,

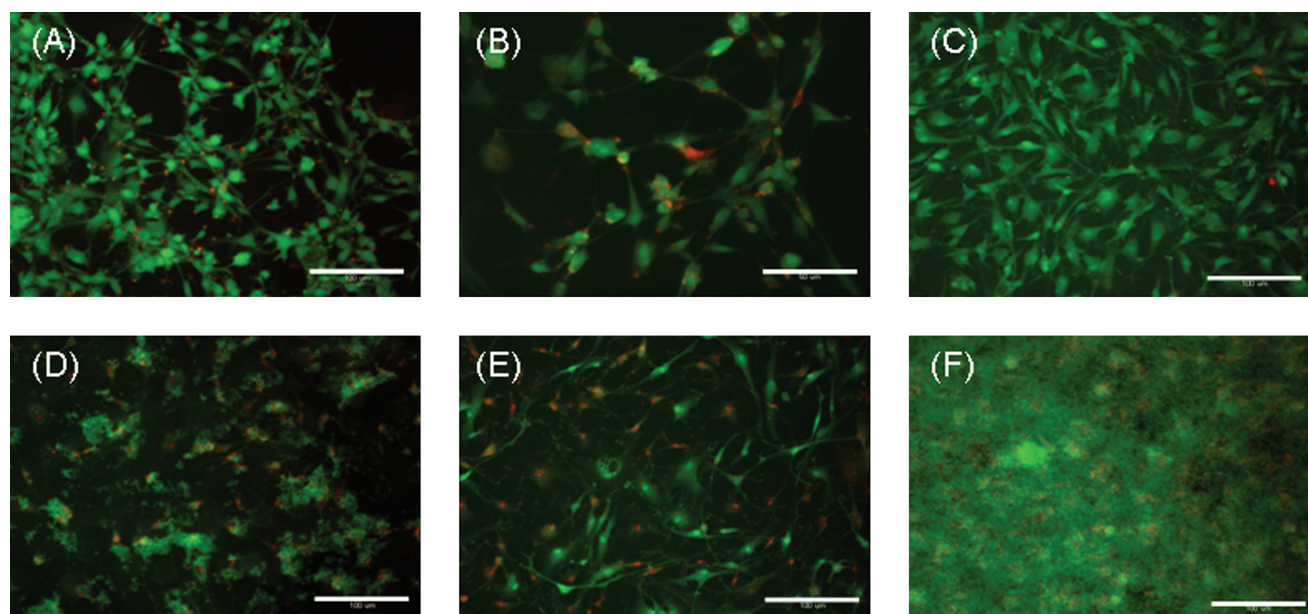


FIG. 6. Fluorescence microscopic images of (A) the synovial cells, and (B–F) the alternately soaked cells with various concentrations of CaCl_2 /50 mM Tris-HCl buffer (pH = 7.4) and Na_2HPO_4 /50 mM Tris-HCl buffer (pH = 7.4). (B) 20 cycles in 10 mM, (C) 10 cycles in 50 mM, (D) 10 cycles in 100 mM, (E) 3 cycles in 200 mM, and (F) 10 cycles in 200 mM buffer. The cells were labeled with calcein-AM and EthD-1 after the alternate soaking process. All scale bars are 100 μm . Color images available online at www.liebertonline.com/ten.

respectively). Statistically significant differences in DNA content were detected after 10 compared to 20 cycles in 200 mM buffer ($p < 0.01$). These results clearly confirmed the cytotoxicity of the calcium and phosphate buffers at concentrations >100 mM. Recently, Maeno *et al.* reported the effects of calcium ion concentrations on osteoblast viability in 2D and 3D cultures.²⁵ They reported that concentrations of calcium ion over 10 mM in the culture media exhibited cytotoxicity for osteoblast cultures after 7 days of incubation. In the present study, although the synovial MSCs in the TEC were immersed in the calcium and phosphate buffers for only 10 s, high concentrations (>100 mM) of calcium buffer showed definite cytotoxicity. Therefore, since the cytotoxicity was not observed at concentrations below 50 mM even after 20 cycles, the TEC-HAp composites with living cells should be developed using low concentrations of calcium and phosphate buffers.

TEC-HAp composite materials with living cells

Based on the above results, 20 cycles of alternate soaking of the TEC using 10 mM calcium/Tris-HCl and phosphate/Tris-HCl buffers were performed to avoid cytotoxicity. Figure 8A and B shows SEM images of the resultant TEC-HAp composite surfaces. Approximately 500-nm-diameter spherical HAp nanocrystals were observed on the surface of the cells and ECM fibers, and the HAp crystals were sparsely distributed on the TEC. However, a very dense deposition of HAp crystals (the size was ca. 1 μm) was observed after 20 cycles at the 200 mM concentration (Fig. 5B). The crystallographic structure of the HAp formed on the TEC under these conditions was confirmed by FT-IR spectroscopy and the WAXD pattern (Fig. 8C, D). These results suggest that the size of the HAp crystals could be controlled by varying

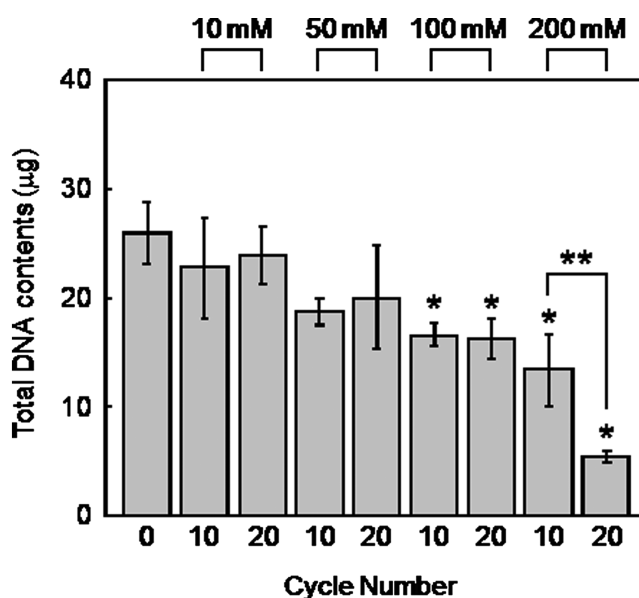


FIG. 7. Total DNA content of the TEC after the alternate soaking process in various concentrations of CaCl_2 /50 mM Tris-HCl buffer (pH = 7.4) and Na_2HPO_4 /50 mM Tris-HCl buffer (pH = 7.4) ($n = 3$). The TEC without any alternate soaking (0 cycle) represents the control. Asterisk (*) indicates statistically significant difference ($p < 0.01$) using a two-sample *t*-test for each comparison with the control. Statistically significant differences in DNA content were detected after 10 versus 20 cycles in 200 mM buffer (** $p < 0.01$).

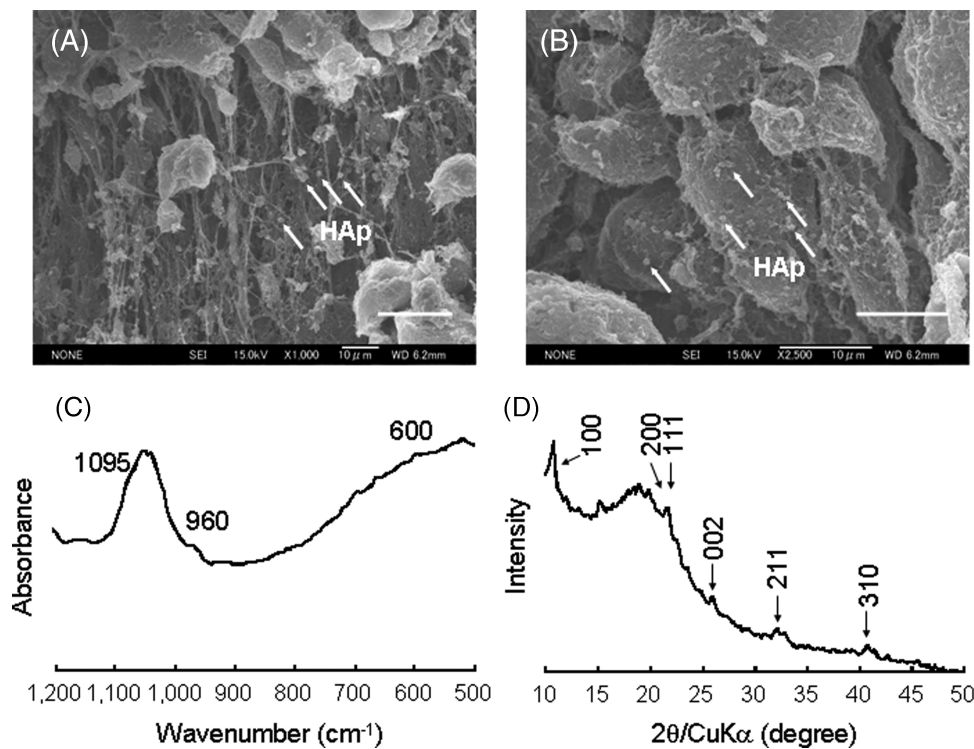


FIG. 8. (A, B) SEM images, (C) FT-IR spectrum, and (D) WAXD pattern of the TEC after 20 cycles of alternate soaking in 10 mM CaCl_2 /50 mM Tris-HCl and Na_2HPO_4 /50 mM Tris-HCl buffers (pH=7.4). In (A) and (B), the arrows indicate HAp crystals. The scale bars are 20 and 10 μm in (A) and (B), respectively.

the concentration of the calcium and phosphate buffers in the alternate soaking process. Since the mean DNA content of the TEC-HAp composite generated with the 20 cycles of the 10 mM buffer was 23.9 μg, approximately the same as the original TEC, the cells were also maintained in a viable state. To visually evaluate the living cells in the TEC-HAp composite, the WST-1 method was used. Figure 9 is a photograph of a TEC-HAp composite stained with WST-1 formazan. The composite was clearly yellow, suggesting that the cells present in the composite are living. These findings indicated that TEC-HAp composites composed of living human synovial

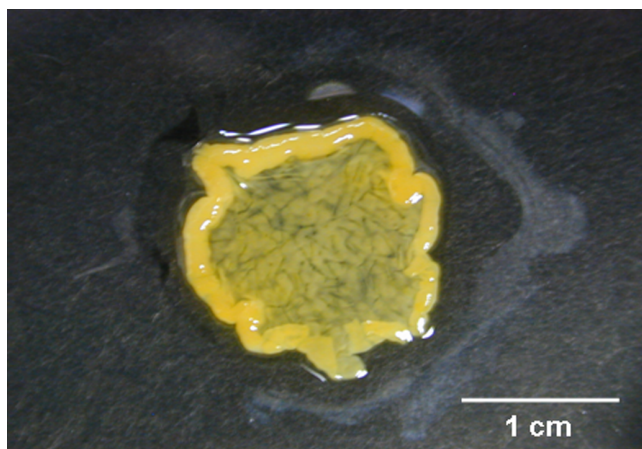


FIG. 9. Photograph of the TEC stained with WST-1 formazan after 20 cycles of alternate soaking in 10 mM CaCl_2 /50 mM Tris-HCl buffer (pH=7.4) and 10 mM Na_2HPO_4 /50 mM Tris-HCl buffer (pH=7.4). Color images available online at www.liebertonline.com/ten.

MSCs, and HAp nanocrystals can be directly formed on the cell surface by optimization of the buffer concentrations.

Early effect of rabbit TEC-HAp on bone repair

Finally, we performed preliminary *in vivo* implantation experiments with rabbit TEC-HAp composites to assess their potential to repair bony defects in the medial femoral condyle of skeletally mature rabbits. When assessed at 6 weeks postsurgery, immediate implantation of basic TEC into defects initiated repair with a resultant fibrous tissue (Fig. 10A, C, and E). Conversely, implantation of TEC-HAp composites clearly induced osteogenesis (indicated by the arrows at the bottom of bone defect sites; Fig. 10B, D, and F). Although the long-term detailed implantation experiments of rabbit TEC-HAp composites are now in progress, the present results strongly suggest that TEC-HAp composites exhibit an enhanced osteoinductive capacity *in vivo* as compared with the basic TEC. Therefore, it is likely that HAp deposition resulted in the enhancement of osteoinduction by the TEC, and thus TEC-HAp composites could be a unique and promising material for bone tissue engineering.

Conclusions

In summary, TEC-HAp composites were successfully developed by an alternate soaking process. Spherical HAp crystals were formed directly on the surface of the synovial MSCs and ECM fibers. Further, the resultant cell viability was controllable by adjusting the concentration of the calcium and phosphate buffers. Moreover, preliminary studies revealed that TEC-HAp composites show definite osteoinduction properties *in vivo*. To the best of our knowledge, this is the first example of a HAp nanocomposite material composed of living MSCs, ECM fibers, and HAp nanocrystals.

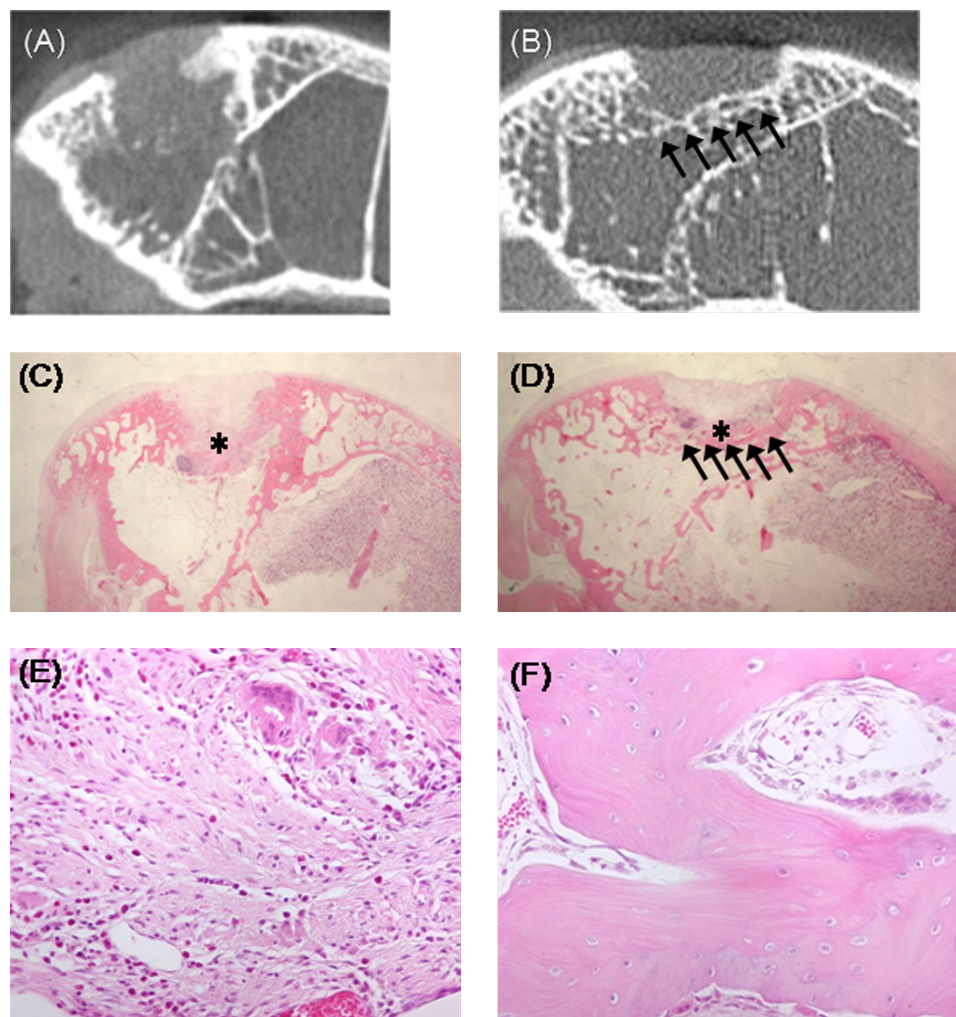


FIG. 10. μ CT and hematoxylin and eosin (HE) staining images of osteochondral defects with (A, C) TEC and (B, D) TEC-Hap composite (20 cycles of alternate soaking in 10 mM CaCl_2 and Na_2HPO_4 buffers) at 6 weeks after implantation. The healing areas are shown with arrows. (E) and (F) are magnified HE images of (C) and (D) at asterisk (*)-marked positions, respectively. Color images available online at www.liebertonline.com/ten.

Further, we have also confirmed that human serum is no less effective than bovine serum in promoting proliferation of synovium-derived MSCs without compromising the differentiation potential of the cells.²⁶ With the use of autologous human serum, it is technically possible to develop xeno-free TEC-Hap composites. Thus, such composites have great potential as a unique, safe, and promising implantable material for bone tissue engineering.

Acknowledgments

This work was financially supported in part by a Grant-in-Aid for Scientific Research B (16390438) from the Ministry of Education, Culture, Sports, Science, and Technology of Japan. This work was also supported by the 21st Century Center of Excellence (COE) program "Center for Integrated Cell and Tissue Regulation" of Osaka University. D.A.H. is the Calgary Foundation–Grace Glaum Professor in Arthritis Research.

References

1. Jarcho, M., Kay, J.L., Cumaer, R.H., and Drobeck, H.P. Tissue, cellular and subcellular events at bone-ceramic hydroxyapatite interface. *J. Bioeng.* **1**, 79, 1977.
2. LeGeros, R.Z., and LeGeros, J.P. Dense hydroxyapatite. In: Hench, L.L., Wilson, J., eds. *An Introduction to Bioceramics*. Singapore: World Scientific, 1993, pp. 140–145.
3. Woo, K.M., Seo, J., Zhang, R., and Ma, P.X. Suppression of apoptosis by enhanced protein adsorption on polymer/hydroxyapatite composite scaffolds. *Biomaterials* **28**, 2622, 2007.
4. Kim, S.-S., Park, M.S., Gwak, S.-J., Choi, C.Y., and Kim, B.-S. Accelerated bonelike apatite growth on porous polymer/ceramic composite scaffolds *in vitro*. *Tissue Eng.* **12**, 2997, 2006.
5. Hutchens, S.A., Benson, R.S., Evans, B.R., O'Neill, H.M., and Rawn, C.J. Biomimetic synthesis of calcium-deficient hydroxyapatite in a natural hydrogel. *Biomaterials* **27**, 4661, 2006.
6. Nge, T.T., and Sugiyama, J. Surface functional group dependent apatite formation on bacterial cellulose microfibrils network in a simulated body fluid. *J. Biomed. Mater. Res.* **81A**, 124, 2006.
7. Kim, H.-W., Kim, H.-E., and Salih, V. Stimulation of osteoblast responses to biomimetic nanocomposites of gelatin-hydroxyapatite for tissue engineering scaffolds. *Biomaterials* **26**, 5221, 2005.
8. Bigi, A., Panzavolta, S., Sturba, L., Torricelli, P., Fini, M., and Giardini, R. Normal and osteopenic bone-derived osteoblast

- response to a biomimetic gelatin-calcium phosphate bone cement. *J. Biomed. Mater. Res.* **78A**, 739, 2006.
9. Punnama, S., Pathavuth, M., Supatra, J., and Khemchai, H. Preparation and characterization of hydroxyapatite/poly(ethylene glutarate) biomaterials. *J. Biomed. Mater. Res.* **81A**, 381, 2007.
 10. Wang, Y., Yang, C., Chen, X., and Zhao, N. Biomimetic formation of hydroxyapatite/collagen matrix composite. *Adv. Eng. Mater.* **8**, 97, 2006.
 11. Honda, Y., Kamakura, S., Sasaki, K., and Suzuki, O. Formation of bone-like apatite enhanced by hydrolysis of octacalcium phosphate crystals deposited in collagen matrix. *J. Biomed. Mater. Res.* **80A**, 281, 2007.
 12. Hubbell, J.A. Materials as morphogenetic guides in tissue engineering. *Curr. Opin. Biotechnol.* **14**, 551, 2003.
 13. Nishikawa, M., Myoui, A., Ohgushi, H., Ikeuchi, M., Tamai, N., and Yoshikawa, H. Bone tissue engineering using novel interconnected porous hydroxyapatite ceramics combined with marrow mesenchymal cells: quantitative and three-dimensional image analysis. *Cell Transplant.* **13**, 367, 2004.
 14. Ando, W., Tateishi, K., Hart, D.A., Katakai, D., Tanaka, Y., Nakata, K., Hashimoto, J., Fujie, H., Shino, K., Yoshikawa, H., and Nakamura, N. Cartilage repair using *in vitro* generated scaffold-free tissue engineered construct derived from porcine synovial mesenchymal stem cells. *Biomaterials* **28**, 5462, 2007.
 15. Taguchi, T., Kishida, A., and Akashi, M. Hydroxyapatite formation on/in hydrogels using a novel alternate soaking process. *Chem. Lett.* **27**, 711, 1998.
 16. Taguchi, T., Kishida, A., and Akashi, M. Apatite formation on/in hydrogels using a novel alternate soaking process (III): effect of physico-chemical factors on apatite formation on/in poly(vinyl alcohol) hydrogel matrix. *J. Biomater. Sci. Polym. Ed.* **10**, 795, 1999.
 17. Tabata, M., Shimoda, T., Sugihara, K., Ogomi, D., Serizawa, T., and Akashi, M. Osteoconductive and hemostatic properties of apatite formed on/in agarose gel as a bone-grafting materials. *J. Biomed. Mater. Res. Part B Appl. Biomater.* **67B**, 680, 2003.
 18. Matsusaki, M., Kamezawa, T., Shimozuru, T., Kuratsu, J.-I., Kishida, A., and Akashi, M. Novel Guglielmi detachable coils (GDCs) for the treatment of brain aneurysms: *in vitro* study of hydroxyapatite coating on Pt plate as GDCs model. *J. Biomed. Mater. Res. Part B Appl. Biomater.* **66B**, 429, 2003.
 19. Tabata, M., Shimoda, T., Sugihara, K., Ogomi, D., Ohgushi, H., and Akashi, M. Apatite formed on/in agarose gel as a bone-grafting material in the treatment of periodontal infrabony defect. *J. Biomed. Mater. Res. Part B Appl. Biomater.* **75B**, 378, 2005.
 20. Kokubo, T. Surface chemistry of bioactive glass-ceramics. *J. Non-Cryst. Solids* **120**, 138, 1990.
 21. Papadopoulos, N.G., Dedoussis, G.V.Z., Spanakos, G.A., Gritzapis, D., Baxevanis, C.N., and Papamichail, M. An improved fluorescence assay for the determination of lymphocyte-mediated cytotoxicity using flow cytometry. *J. Immunol. Methods* **177**, 101, 1994.
 22. Mosmann, T. Rapid colorimetric assay for cellular growth and survival: application to proliferation and cytotoxicity assays. *J. Immunol. Methods* **65**, 55, 1983.
 23. Okamoto, M., Murai, J., Yoshikawa, H., and Tsumaki, N. Bone morphogenetic proteins in bone stimulate osteoclasts and osteoblasts during bone development. *J. Bone Miner. Res.* **21**, 1022, 2006.
 24. Arimura, S., Kawahara, K.-I., Biswas, K.K., Abeyama, K., Tabata, M., Shimoda, T., Ogomi, D., Matsusaki, M., Kato, S., Ito, T., Sugihara, K., Akashi, M., Hashiguchi, T., and Maruyama, I. Hydroxyapatite formed on/in agarose gel induces activation of blood coagulation and platelets aggregation. *J. Biomed. Mater. Res. Part B Appl. Biomater.* **81B**, 456, 2007.
 25. Maeno, S., Niki, Y., Matsumoto, H., Morioka, H., Yatabe, T., Funayama, A., Toyama, Y., Taguchi, T., and Tanaka, J. The effect of calcium ion concentration on osteoblast viability, proliferation and differentiation in monolayer and 3D culture. *Biomaterials* **26**, 4847, 2005.
 26. Tateishi, K., Ando, W., Higuchi, C., Hart, D.A., Hashimoto, J., Nakata, K., Yoshikawa, H., and Nakamura, N. Comparison of human serum with fetal bovine serum for expansion and differentiation of human synovial MSC: potential feasibility for clinical applications. *Cell Transplant.* (in press).

Address reprint requests to:
 Norimasa Nakamura, M.D., Ph.D.
 Department of Orthopaedics
 Graduate School of Medicine
 Osaka University
 2-2 Yamada-oka
 Suita 565-0871
 Japan

E-mail: n-nakamura@ort.med.osaka-u.ac.jp

Received: December 18, 2007

Accepted: April 23, 2008

Online Publication Date: July 31, 2008